NeuroImage 201 (2019) 116053

Contents lists available at ScienceDirect

NeuroImage

journal homepage: www.elsevier.com/locate/neuroimage

The dorsomedial prefrontal cortex as a flexible hub mediating behavioral as well as local and distributed neural effects of social support context on pain: A Theta Burst Stimulation and TMS-EEG study

Xianwei Che [a,*], Robin Cash [a], Sung Wook Chung [a], Neil Bailey [a,b], Paul B. Fitzgerald [a,b], Bernadette M. Fitzgibbon [a]

[a] Monash Alfred Psychiatry Research Centre (MAPrc), The Alfred and Central Clinical School, Monash University, Melbourne, Australia
[b] Epworth Centre for Innovation in Mental Health, Epworth, VIC, Australia

ARTICLE INFO

Keywords:
Social support
Pain
Theta burst stimulation
TMS-EEG
Connectivity

ABSTRACT

Increasing evidence points to an analgesic influence of social support context, in which the dorsomedial prefrontal cortex (dmPFC) may play a key role. Transcranial Magnetic Stimulation (TMS) has the capacity to causally modulate brain activity. This study was designed to investigate the potential role of dmPFC in orchestrating the behavioral and neural effects of social context during pain. Twenty-three healthy participants underwent a three-session cross-over, single-blinded, sham-controlled protocol in which they received Theta Burst Stimulation (TBS) (facilitatory intermittent TBS, suppressive continuous TBS, or Sham) delivered to the dmPFC. In each session, participants underwent cold pain while viewing an image of a romantic partner or a stranger. Effects of TBS to the dmPFC were assessed using a measure of pain perception, neural activity and network connectivity using electroencephalography (EEG) and TMS-EEG. In the stranger condition, pain experience increased following iTBS. This was associated with increased connectivity between central regions and fronto-parietal regions. In contrast, in the romantic partner condition, iTBS increased connectivity only between frontal and occipital regions and did not modulate pain experience. In line with recent studies, neither cTBS nor Sham stimulation elicited neural or behavioral changes. Together these findings suggest that the dmPFC has the capacity to causally modulate pain-related information integration and network configuration in a context-dependent manner.

1. Introduction

Pain experience is modulated by a variety of social contexts in daily life (for review see Krahé et al., 2013). Emerging evidence has suggested an analgesic influence of social support (Che et al., 2017, 2018b; Goldstein et al., 2016), which commonly refers to received support from others and the perceived availability of supportive resources (Dunkel-Schetter and Bennett, 1990). However, recent systematic reviews, including one meta-analysis from our group, have demonstrated that this effect is not universal and highlighted the role of contextual factors (Che et al., 2018a; Krahé et al., 2013). Indeed, social support from a significant other can prime intimacy and reduce pain, but the presence of another person in general may not have an overall effect (for a review see Che et al., 2018a).

Advancing our understanding of the role of social support in pain therefore requires improved knowledge of the mechanisms that mediate the impact of social support on pain. Initial evidence suggests a role of social support in priming feelings of attachment, as supported by increased brain activity (blood-oxygen-level dependent imaging, BOLD) in the medial prefrontal cortex (mPFC) (Eisenberger et al., 2011; Younger et al., 2010). Increased activity in the mPFC, including the dorsomedial prefrontal cortex (dmPFC), has been extensively observed in the processing of social intimacy (Gamond and Cattaneo, 2016; Gamond et al., 2017) and inferring the purpose of others' actions (Bzdok et al., 2012; Schuwerk et al., 2014). Moreover, the dmPFC is part of the default mode network (DMN) (Fox et al., 2005), which is associated with self-report of perceived social support (Che et al., 2014) and mind wandering away from pain (Kucyi et al., 2013). In fact, the dmPFC is implicated in a number of processes relevant to the modulation and perception of pain (Apkarian et al., 2005; Peyron et al., 1999). For example, the dmPFC has been associated with the selective attention to nociceptive stimuli (Peyron et al., 1999) and the cognitive load linked to ratings of body

* Corresponding author. Monash Alfred Psychiatry Research Centre (MAPrc), Monash University, Level 4, 607 St Kilda Road, Melbourne, VIC, 3004, Australia.
E-mail address: xianwei.che@monash.edu (X. Che).

https://doi.org/10.1016/j.neuroimage.2019.116053
Received 18 December 2018; Received in revised form 18 July 2019; Accepted 23 July 2019
Available online 24 July 2019

sensations (Napadow et al., 2009). However, previous evidence has been primarily correlational, and therefore restricted in its capacity to assess the causal relationships of the dmPFC in facilitating the processing of social support and its impact on pain. Moreover, the brain-wide dynamics that mediate the influence of social support on pain remain to be elucidated.

Transcranial Magnetic Stimulation (TMS) is a non-invasive approach which can modulate brain activity, and thereby provide unique insights into brain-behavior relationships. Theta Burst Stimulation (TBS) is one of the most established repetitive TMS protocols and has the capacity to modulate neural excitability (Huang et al., 2005; Ni et al., 2014) and network connectivity (Iwabuchi et al., 2017; Rastogi et al., 2017). More specifically, intermittent TBS (iTBS) is designed to increase cortical excitability while continuous TBS (cTBS) decreases excitability (Huang et al., 2005). Thus, TBS provides a means to causally modulate the dmPFC and its associated networks and explore the role of this brain region in the effects of social support on pain. In addition, changes in neural activity induced by TBS can be measured using single-pulse TMS and concurrent electroencephalography (TMS-EEG) (Cash et al., 2017; Chung et al., 2017). Of note, recent studies suggest that iTBS may be more effective than cTBS in modulating brain activity when applied to the prefrontal cortex (Berlim et al., 2017; Chung et al., 2017).

Changes in EEG activity and connectivity following TBS may help to reveal regional and network-based neural mechanisms that mediate the influence of social support on pain. Although the frequency dynamics of the experience of pain are not entirely understood (Ploner et al., 2017), with each of the bands implicated (e.g. for alpha see Furman et al., 2018), most studies link subjective pain ratings with increased gamma activity (31–100 Hz) in central and frontal cortex (Nickel et al., 2017; Schulz et al., 2015; Zhang et al., 2012). To our knowledge, only one EEG study has explored phase synchronization in response to painful stimuli, which found increased theta range (4–7 Hz) connectivity between central and parietal regions (Taesler and Rose, 2016). Additionally, only one study examined EEG connectivity in the context of social influence on pain, which indicated that increased alpha band (8–12 Hz) connectivity was associated with the analgesic effects of social touch on pain (Goldstein et al., 2018).

The present study was designed to investigate the role of the dmPFC in mediating the effects of social support on pain. Participants underwent a three-session cross-over, single-blinded, sham-controlled protocol in which they received either iTBS, cTBS, or Sham stimulation. A pain task was performed before and after TBS during which participants were subjected to cold pain while viewing an image of either a romantic partner or a stranger (Eisenberger et al., 2011). Viewing these images has previously been shown to reflect social support priming feelings of attachment to reduce pain (Eisenberger et al., 2011).

Overall, we anticipated that modulation of dmPFC activity using iTBS would affect the interaction between social support and pain perception. More specifically, we hypothesized that iTBS would increase neural activity in the prefrontal cortex (assessed using TMS-EEG) and that in the romantic partner condition, iTBS would increase social support related alpha connectivity and reduce pain related gamma power, theta connectivity, and pain sensation. In contrast, we hypothesized no changes in the stranger condition. We also anticipated less pronounced and potentially opposite changes in the sham and cTBS sessions.

2. Methods

2.1. Participants

Twenty-three healthy right-handed adults participated in this study. Three participants withdrew after the first session. Data from 20 participants were therefore analyzed (see Table 1). Exclusion criteria included a history or current diagnosis of a psychiatric disorder, or use of psychoactive medication, as assessed by the Mini International Neuropsychiatric Interview (MINI) (Sheehan and Lecrubier, 2001). All participants identified as being in a romantic relationship. An informed consent was provided by all participants, and the experiment was approved by the Alfred Hospital and Monash University Human Research and Ethics Committee. This study was conducted in accordance with the Declaration of Helsinki.

Table 1
Descriptive characteristics of the sample.

	Sample size	Mean	Standard deviation
Gender	8 (M), 12 (F)	–	–
Age	20	26.45	4.54
BDI	20	2.2	2.46
STAI-Y2		36.5	6.47
MSPSS		6.03	0.82
PCS		12.9	9.39
DAS		117.55	10.15
ECR-R: anxiety		2.26	0.82
ECR-R: avoidance		2.13	0.77

M–male; F–female; BDI–The Beck Depression Inventory; STAI-Y2–The State Trait Anxiety Inventory-trait; MSPSS–The Multidimensional Scale of Perceived Social Support; PCS–The Pain Catastrophizing Scale; DAS–Dyadic Adjustment Scale; ECR-R–The Experiences in Close Relationships-Revised.

2.2. Experimental design and procedure

Participants underwent a three-session data collection protocol with each session at least 72 h apart to avoid any potential carry-over effects (Fig. 1). The experimental procedures were the same in each of the three sessions except for the type of TBS protocol (i.e. iTBS, cTBS or Sham), the order of which was counterbalanced across participants. During the first session participants completed several self-report questionnaires (see Table 1). In each session, participants first underwent a 3-min pain protocol with EEG recorded to assess neural oscillations and connectivity. In the pain protocol, participants viewed an image of either a stranger or their romantic partner (in total 2 separate trials), and rated pain at 20-s intervals for the 3 min. Next, single-pulse TMS was delivered to the dmPFC and cortical responses were recorded using concurrent EEG. Participants then received either iTBS, cTBS or Sham stimulation to the dmPFC, which was followed by a repeat of the pain and TMS-EEG protocol described above.

2.3. Social support or stranger attachment image

Consistent with a template image (i.e. the gender-matched stranger image), a digital image of the romantic partner was taken by the participants and provided for the study. Specifically, the image was requested to be against a plain white background, demonstrating a natural smile and including only the head and shoulders. One of the researchers (XC) then edited the images (GNU Image Manipulation Program, GIMP, V2.8) to have the fixed size (17.5 cm × 17.5 cm), content (from the top of head to shoulders), and matched for luminance using the "auto adjust color levels" function (Parsons et al., 2013). Two images, one male and one female in early adulthood, served as the stranger images.

2.4. Pain protocol

In order to control baseline hand temperature (Hadjileontiadis, 2015), participants were asked to insert their dominant hand into a bucket of warm water (40 °C ± 0.2 °C) for 2 min and relax for another 5 min prior to and between experimental trials. Participants were then asked to hold a bottle filled with iced water (−1 °C ± 0.2 °C) for 3 min (i.e. a single trial) with the dominant hand (Hadjileontiadis, 2015). A trial was started by pressing a button with the non-dominant hand in the keypad. The button press started the presentation of an image (Presentation, Version 17.0, Neurobehavioral Systems, Berkeley, CA), which was

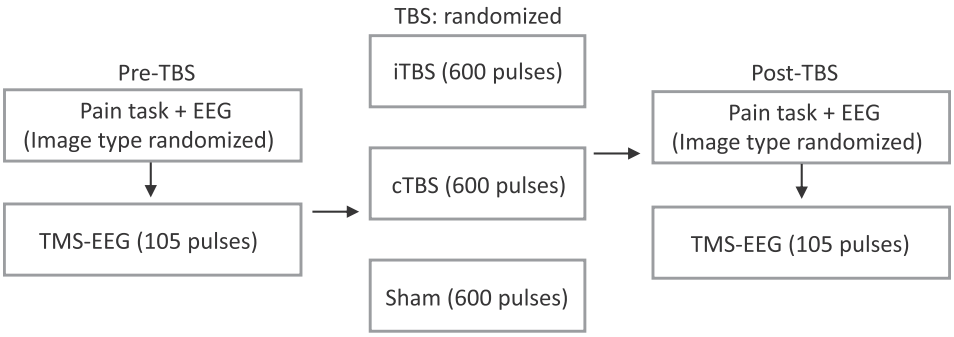

Fig. 1. Experimental procedure. This was the experimental procedure for each session.

either their romantic partner or a stranger matched to the partner's gender (Eisenberger et al., 2011). These two conditions were performed separately in two trials, and the order of conditions was pseudorandomized and counterbalanced across participants. A 3-min trial was divided into nine 20-s blocks during which the participants viewed the image for 16 s and then rated pain intensity within 4 s. The participants were asked to rate "pain intensity at the moment" on a scale of 0–10 (0 = no pain; 10 = worst pain imaginable), by pressing the corresponding button on a keypad. At the end of the trial, participants rated their "overall perceived support" from the image by pressing the corresponding button (0 = not at all; 10 = extremely high). A pillow was provided on which participants rested the back of their hands to avoid hand movement. Participants were told to put the volar surface of the dominant hand on the surface of the ice bottle. They were asked not to squeeze the bottle and to ensure they maintained contact with the bottle throughout. Fresh ice bottles were used for each experimental trial for consistency.

2.5. EEG recordings

EEG recordings took place in a temperature-controlled, sound-attenuated, and electrically shielded room. Participants were seated in a slightly reclined chair with their faces approximately 0.5 m from the computer monitor. A 64-channel EEG cap (NeuroScan Inc., Australia) was used to record continuous EEG with CPZ and FPZ as the reference and ground electrode respectively. Two electrodes were attached above and below the left eye to monitor vertical electrooculogram (EOG) activity. Horizontal EOG activity was monitored with electrodes located at the outer canthus of both eyes. EEG impedances were kept below 5 kΩ throughout the experiment.

For EEG recordings during the pain protocol, EEG signals were filtered (0.05–200 Hz) and sampled at 1000 Hz. For TMS-EEG recordings, EEG signals were amplified (1000 ×) and low-pass filtered (DC—2000 Hz) with a high acquisition rate of 10,000 Hz. As the TMS click sound might contaminate the EEG signals (Nikouline et al., 1999), participants were asked to listen to white noise through intra-auricular earphones (Etymotic Research, ER3-14A, USA) during TMS-EEG recordings (Fuggetta et al., 2005). The sound level was adjusted such that each individual reported that they could no longer hear single-pulse TMS at 110% resting motor threshold (RMT).

2.6. Transcranial Magnetic Stimulation

Both single-pulse TMS and TBS were delivered using a figure-of-eight MagVenture B-65 fluid-cooled coil (MagVenture A/S, Denmark) in a biphasic mode. In the determination of the RMT, stimuli were applied to the left motor cortex with the coil positioned at 45° angle relative to midline (Chung et al., 2018b, 2018c). The RMT was determined with the EEG cap on, as the minimum stimulus intensity required to elicit at least three out of five motor evoked potentials (MEPs) > 0.05 mV in amplitude in the relaxed first dorsal interosseous muscles (Conforto et al., 2004). Prefrontal TMS was then administered, with the coil centred at the F1 electrode. This electrode was selected as it is positioned over the superior frontal gyrus (Koessler et al., 2009). The left hemisphere was targeted due to previous evidence of the analgesic influence of social support associated with increased activity in the left mPFC(Eisenberger et al., 2011; Younger et al., 2010). The coil was positioned at 90° angle relative to midline (handle pointing left, see Fig. 2a) in order to target the dmPFC (Downar et al., 2012; Salomons et al., 2014). The edge of the TMS coil was marked on the EEG cap for consistent re-positioning of the coil within and between sessions (Rogasch et al., 2013). The TMS-evoked potentials (TEPs) were recorded using EEG during single-pulse TMS (105 pulses, 4 s interval ± 10% jitter) at 110% RMT, delivered before and after TBS. TBS consisted of a burst of 3 pulses given at 50 Hz repeated every 5 Hz, where (1) iTBS involved a 2s train of TBS repeated every 10s for a total of 192s, (2) cTBS without any break/interruption for a total of 40s, or (3) Sham – the iTBS protocol was administrated using a MagVenture Placebo B-65 coil which has a sound level identical to the B-65 coil. TBS was delivered with the intensity of 70% RMT (Goldsworthy et al., 2012), with a total of 600 pulses. A 5-min break was included after TBS administration (Chung et al., 2018a, 2018b).

In order to validate the target site, electric field simulations for the cooled B-65 TMS coil (90° angle) were performed using the SimNIBS modelling environment, which utilizes a finite element model of brain current flow based on an MRI derived template head model (Windhoff et al., 2013). Visualization of the electrical fields was performed using the Gmsh mesh generator (Geuzaine and Remacle, 2009).

2.7. EEG data analysis

EEG data during the pain protocol were preprocessed offline using custom-written scripts that implement functions from EEGLAB (version 13.6.5b) (Delorme and Makeig, 2004) running under Matlab R2017b (The MathWorks, Inc.). Data from malfunctioning channels were visually inspected and removed. Butterworth filters (band-pass: 0.5–100 Hz; band-stop notch filter: 48–52 Hz) were then applied to the data (Selesnick and Burrus, 1998). Continuous data were segmented to retain only the image viewing stage, i.e. 16 s in each block, in total 9 in each 3-min pain stimulation trial. Data were further segmented into 1-s non-overlapping epochs to remove any contaminated data (Peng et al., 2014; Schulz et al., 2015). Segmented data were re-referenced to the average reference, and the fast independent component analysis algorithm (FastICA) was used to remove stereotyped artefacts, e.g. eye blinks, lateral eye movements, muscle, and line noise (Korhonen et al., 2011). Stereotyped artefacts were identified by visual inspection of the temporal and spatial representation of the independent components. Missing channels were then interpolated, and epochs were inspected again to remove any anomalous activity in the signal. Rejected channels were no more than three in each dataset, and the final trial numbers were as follows (averaged across sessions, Mean ± SD): Pre_Partner: 135.07 ± 8.90; Pre_Stranger: 136.77 ± 6.74; Post_Partner: 137.12 ± 6.79; Pre_Stranger: 137.33 ± 5.71.

EEG frequency representations were calculated with the Multitaper Method Fast Fourier Transform ('mtmfft'), as implemented in FieldTrip

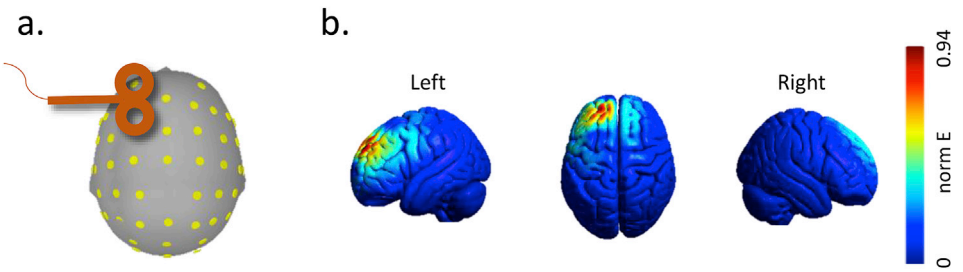

Fig. 2. TMS delivery and electric field modelling of the study. (a) Both single-pulse and TBS were delivered to the F1 electrode in the 10–20 system. (b) Distribution of the induced normalized electric field (norm E) with maximal activation at the left mPFC.

toolbox, in the range of 0.5–100 Hz (Oostenveld et al., 2011). Power spectra were calculated for each epoch, and then averaged across epochs in each condition.

EEG connectivity was calculated between each electrode using the debiased estimator of the weighted phase lag index (wPLI) based on the frequency representations obtained above. The wPLI is considered as a conservative measure of phase synchronization, which is suggested to be robust against volume conduction, non-brain related artefacts and common reference artefacts (Vinck et al., 2011). The measure also has good test-retest reliability (Hardmeier et al., 2014). For each frequency, the wPLI provided a value of coherence for each electrode pair. Connectivity values were then averaged in the frequency domains of interest, i.e. theta (4–7 Hz) (Taesler and Rose, 2016), or alpha (8–12 Hz) (Goldstein et al., 2018). Exploratory analyses were also performed in other frequency bands (i.e. delta: 1–3 Hz; beta: 13–30 Hz; gamma: 31–100 Hz).

2.8. TMS-EEG data analysis

TMS-EEG data were preprocessed as previously described (Chung et al., 2017). Specifically, data were epoched around the TMS pulses (−1000 to 1000 m s), baseline corrected (−500 to −50 m s), and then the large magnetic pulses were removed and interpolated (−5–15 m s). Data were down-sampled to 1000 Hz and epochs containing excessive noise and/or disconnected electrodes were removed during manual inspection. Prior to independent component analysis (ICA) based artefact rejection, the epoched data were concatenated across the two time-points (Pre and Post) to avoid bias in component rejection. Two rounds of FastICA were performed using semi-automated component classification algorithm (Rogasch et al., 2017). The first ICA was performed to remove large TMS-evoked muscle artefacts and decay artefact (Rogasch et al., 2014). All data were band-pass (1–80 Hz) and band-stop filtered (line noise removal, 48–52 Hz), and epochs were visually inspected again to remove any anomalous activity. The second round of ICA was used to remove other non-neural artefacts, e.g. eye blinks, saccadic movement, persistent muscle activity, decay artefact and electrode noises. Removed channels were then interpolated. Finally, data were re-referenced to common average and segregated into original time-point blocks (Pre and Post) and epochs averaged for each condition. The final pulse numbers were (Mean ± SD): Pre_iTBS: 97.25 ± 2.19; Pre_cTBS: 96.40 ± 4.58; Pre_Sham: 96.95 ± 3.22; Post_iTBS: 97.50 ± 3.10; Post_cTBS: 97.25 ± 3.51; Post_Sham: 97.35 ± 3.54.

2.9. Source estimation

Cortical sources of the TEPs were estimated using Brainstorm (Tadel et al., 2011). TMS-EEG data were co-registered with the template brain model (i.e. ICBM 152). The forward model used the Symmetric Boundary Element Method implemented in OpenMEEG software (Gramfort et al., 2010), and the inverse model used the computation of minimum norm estimations (MNEs) with dipole orientations constrained to be normal to the cortex (Lin et al., 2006). Differences in estimation were calculated using absolute subtraction.

2.10. Statistical analyses

Statistical analyses were performed on the primary outcome measures (self-reported pain ratings, TEPs, EEG power and connectivity).

Pain intensity ratings across 3-min blocks were summarized by calculating the area under the curve (AUC). The effects of TBS and time as well as their interaction were analyzed using repeated measures two-way ANOVAs in SPSS (version 23; IBM Corp, Armonk, NY). The partner and stranger condition were examined separately. TBS (iTBS, cTBS or Sham) and time (Pre, Post) were specified as the two repeated measures factors. Post-hoc pairwise comparisons were conducted to further explore the significant main and interaction effects, with the α-level set to 0.05 and Bonferroni corrected.

For TEPs, statistical analyses were conducted using cluster-based permutation statistics at a global scalp level (Maris and Oostenveld, 2007). The cluster-based permutation test provides a straightforward way to solve the problem of multiple comparisons across space (EEG channels) and time (Maris and Oostenveld, 2007). Statistics were performed on a priori peak of interest (i.e. N100: 90–130 m s), which is considered to be the most prominent and robust TMS-EEG component for the exploration of TMS induced plasticity changes (Chung et al., 2015; Nikulin et al., 2003). Exploratory analyses were also performed on other peaks: N40 (30–50 m s), P60 (50–80 m s), and P200 (160–240 m s), which have been commonly observed following prefrontal stimulation (Chung et al., 2017; Rogasch et al., 2014). Paired T-tests were first made across time point (Post vs Pre) for each TBS condition ('within-comparison'). Comparisons between TBS conditions ('between-comparison') were then performed using delta score of each TBS condition (Δ = Post–Pre). An observed test statistics value was considered in the cluster permutation if it was below the threshold of 0.05 in at least 2 of the neighboring channels (Oostenveld et al., 2011). We performed 5000 iterations of trial randomization for generating the permutation distribution, controlling for multiple comparisons across space ($P < 0.025$; two-tailed test).

For EEG power changes, the same cluster-based permutation statistics were used to identify differences in neural oscillatory activity. This method was applied to each 1-s time window across all channels. Comparisons were made between Pre- and Post-stimulation for each TBS (iTBS, cTBS or Sham) and image (partner, stranger) condition. According to our a priori hypothesis, statistical analyses were firstly carried out in alpha (8–12 Hz), theta (4–7 Hz) and gamma (31–100 Hz) bands. Additional exploratory analyses were performed separately in other frequency bands (i.e. delta: 1–3 Hz; beta: 13–30 Hz).

Connectivity wPLI values were statistically tested using the network-based statistic (NBS) toolbox (Zalesky et al., 2010). The NBS is a non-parametric statistical method which uses cluster analysis to perform null hypothesis testing across networks of values from pairs of potentially connected nodes (Zalesky et al., 2010). It is robust against unequal sample sizes and controls for the family-wise error rate (Zalesky et al., 2010). Paired T-tests were performed to examine significant connectivity changes from Pre-to Post-stimulation for each TBS (iTBS, cTBS, Sham) condition. Statistical comparisons were made using 5000 permutations,

with a primary threshold for electrode pairs set at $P < 0.005$ to ensure only robust differences in connectivity between electrode pairs would be compared at the cluster level (Bailey et al., 2018). The secondary threshold for family-wise corrected cluster null hypothesis testing was $P < 0.025$ (two-tailed).

Correlation analysis was performed to examine brain-behavior relationships between TBS-induced changes in pain ratings and significant TBS-induced changes in EEG power and TEP amplitude.

2.11. Supplementary analyses

In order to demonstrate the baseline differences in pain ratings and overall perceived support between social support conditions, repeated measures two-way ANOVAs were performed for Pre-TBS pain ratings and overall perceived support separately. TBS (iTBS, cTBS or Sham) and image (partner, stranger) were specified as the two repeated measures factors. Post-hoc pairwise comparisons were conducted with the α-level set to 0.05 and Bonferroni corrected.

As iTBS showed distinct effects in the romantic partner and stranger condition, we further explored whether there were differences between these conditions following iTBS. A repeated measures two-way ANOVA was performed on pain ratings with TBS (iTBS, cTBS or Sham) and image (partner, stranger) being specified as the two repeated measures factors and Bonferroni corrected in the Post-hoc pairwise comparisons.

In the romantic partner and stranger condition, repeated measures two-way ANOVAs were performed to examine the changes in overall perceived support, with TBS (iTBS, cTBS or Sham) and time (Pre, Post) being specified as the repeated measures factors.

3. Results

The effectiveness of TBS over the dmPFC was initially validated before the investigation of outcome measures. Fig. 2b shows the electric field distribution in the cortical grey matter for the cooled B-65 coil. The TMS coil effectively targeted the left prefrontal cortex, with maximum field strengths occurring around the left dmPFC. Moreover, single-pulse TMS over left dmPFC resulted in a series of negative and positive peaks including N40, P60, N100 and P200 (*Supplementary Material S1*). Consistent with other TMS-EEG studies in the prefrontal cortex (Chung et al., 2018c; Hill et al., 2017), each peak showed a distinctive pattern in scalp topography and source estimation.

3.1. Effects of TBS on pain intensity ratings

In the partner condition, the ANOVA revealed no effect of TBS protocol, time, or their interaction on pain ratings ($P_s > 0.05$), suggesting that pain ratings were the same across stimulation type and time window (Fig. 3a–d). In the stranger condition (Fig. 3e–h), the ANOVA revealed an interaction effect of TBS protocol and time on pain ratings ($F_{2,38} = 3.51$, $P = 0.04$, $\eta_p^2 = 0.16$). Post-hoc tests were performed to investigate this interaction. Two one-way ANOVAs (one for Pre, one for Post) were first performed across TBS conditions, which were followed by three paired T-tests (one for each TBS condition) conducted across time windows. One-way ANOVAs revealed no effect of TBS on pain ratings in either time window ($P_s > 0.05$), suggesting that pain ratings were the same across TBS conditions in both Pre- and Post-stimulation (Fig. 3e–h). Across time windows, paired T-tests showed a significant increase in pain ratings from Pre-to Post-iTBS ($P_{Bonf} = 0.003$) (Fig. 3e and h). No difference was observed in the cTBS (Fig. 3f) or Sham (Fig. 3g) condition ($P_{Bonf} > 0.05$).

3.2. Plastic effects of TBS on TEPs

Cluster-based permutation tests revealed that the amplitude of the primary TEP component of interest, N100, was significantly increased from Pre-to Post-iTBS ($P_{corrected} = 0.011$) (Fig. 4a). Moreover, the topography of this change was mainly distributed around the frontal regions where iTBS was delivered (Fig. 4d *left panel*). In line with recent evidence (Chung et al., 2017), there were no changes in N100 amplitude following cTBS (Fig. 4b) or Sham (Fig. 4c) ($P_{corrected} > 0.05$). Changes in N100 amplitudes were not associated with increased pain in the stranger condition from Pre-to Post-iTBS ($P > 0.05$). Individual data of N100 was provided in *Supplementary Material S2*.

These findings were supported by secondary analyses in which N100 amplitude Pre-to Post-stimulation was compared across all TBS conditions using permutation tests. Relative to Sham, N100 changes from Pre-to Post-stimulation were significantly larger in the iTBS condition ($P_{corrected} = 0.006$). Moreover, changes in N100 were mainly distributed around the fronto-central regions (Fig. 4d, *right panel*). No difference was found in the iTBS versus cTBS or the cTBS versus Sham comparisons.

3.3. Effects of TBS on EEG oscillations in the pain protocol

In the partner condition, cluster-based permutation statistics revealed

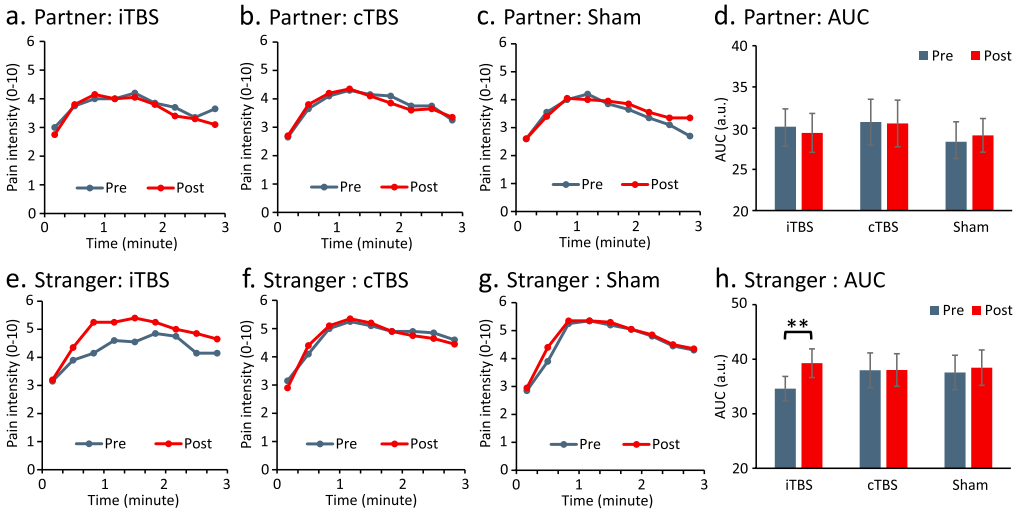

Fig. 3. Pain ratings modulated by different TBS protocols. In the romantic partner condition, (a)–(c) show no effects of iTBS, cTBS, or Sham stimulation on pain ratings across the 3-min pain task. (d) represents the area-under-curves (AUCs) of pain ratings across the pain task. In the stranger condition, (e)–(g) show the pain ratings across the pain task and (g) represents the AUC of pain dynamics. Stranger condition was associated with more pain from Pre-to Post-iTBS. ** indicates $P < 0.01$.

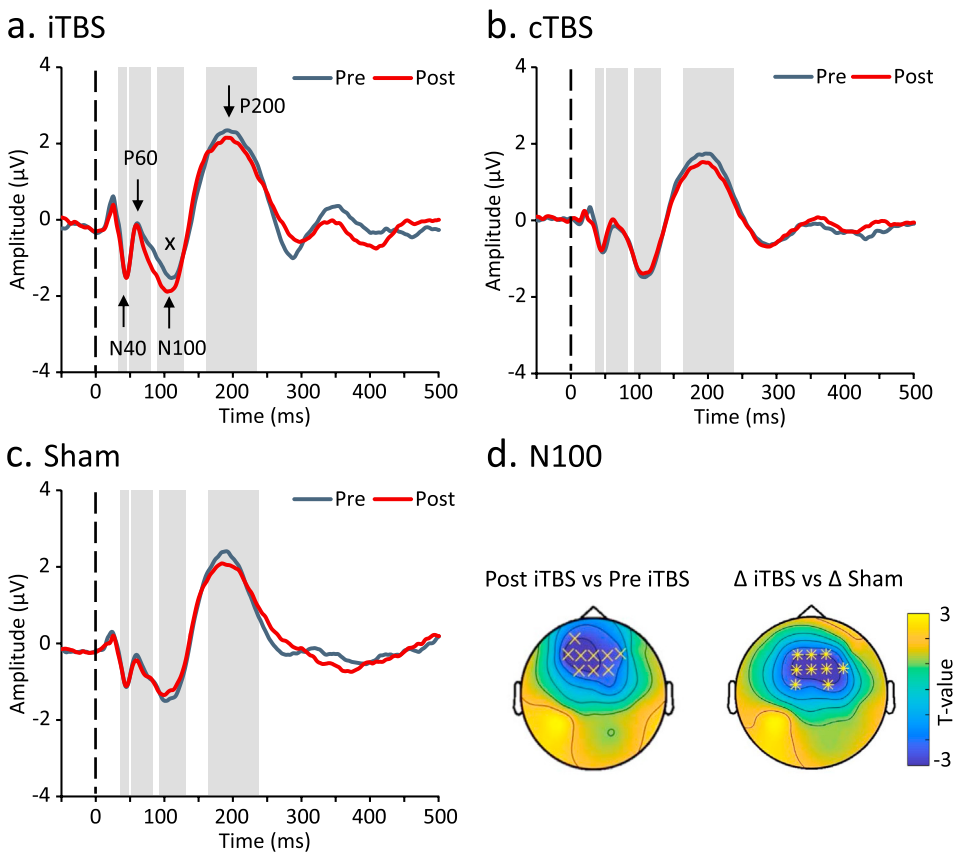

Fig. 4. Modulation of cortical activity assessed via TEPs following different TBS protocols. Grand average TEP waveforms from the three fronto-central electrodes (FC1, FCZ and FC2) for (a) iTBS, (b) cTBS and (c) Sham conditions. iTBS resulted in a larger N100 amplitude from Pre-to Post-stimulation. (d) Scalp maps represent the comparison between iTBS-induced N100 from Pre-to Post-stimulation (*left panel*), and between iTBS-induced N100 change and Sham-induced N100 change (*right panel*). X indicates $P < 0.05$, * indicates $P < 0.01$.

a significant increase in gamma power from Pre-to Post-iTBS ($P_{corrected} = 0.024$). The topography of this power increase had a fronto-central, right-lateralized distribution (significant at F4, F6, FC4, FC6, and C4) (Fig. 5a). The increase in gamma power was associated with larger N100 amplitude from Pre-to Post-iTBS ($r = -0.49$, $P = 0.03$) (Fig. 5a). No correlation was found between gamma changes and pain rating changes ($P > 0.05$). No difference was found in any other frequency bands.

In the stranger condition, we also found increased gamma power from Pre-to Post-iTBS ($P_{corrected} = 0.019$). Increased gamma in the stranger condition was mainly distributed in the left central-parietal regions (significant at T7, C5, C3, CP5, P7, P5 and O1) (Fig. 5b). However, no correlation was found between gamma changes and N100 amplitude or pain ratings changes ($P_s > 0.05$). No difference was found in any other frequency bands.

Following Sham stimulation, alpha activity was greater in both the partner and stranger condition. Moreover, in both the partner ($P_{corrected} = 0.006$) and stranger ($P_{corrected} = 0.021$) condition, increased alpha was mainly distributed in the central regions (Fig. 5c and 5d).

3.4. Effects of TBS on EEG connectivity in the pain protocol

In the partner condition, we found a significant cluster in the alpha band which indicated higher fronto-occipital alpha connectivity from Pre-to Post-iTBS ($P_{corrected} = 0.019$) (Fig. 6a). In the stranger condition, there was an increase in central-parietal and central-frontal theta connectivity from Pre-to Post-iTBS ($P_{corrected} = 0.003$) (Fig. 6b). No other significant clusters were observed in other frequency domains and no significant clusters were observed in the cTBS or Sham stimulation.

3.5. Supplementary analysis

At baseline, the ANOVA revealed a main effect of image on pain ratings ($F_{1,19} = 24.75$, $P = 0.001$, $\eta_p^2 = 0.57$). Post-hoc t-tests indicated that pain ratings were significantly lower when viewing a romantic partner compared to a stranger ($P_{Bonf} = 0.001$). No other effect was observed ($P_s > 0.05$), in other words, this finding was consistent across conditions. Similarly, the ANOVA revealed a main effect of image on overall perceived support ($F_{1,19} = 49.82$, $P = 0.001$, $\eta_p^2 = 0.72$), with post-hoc tests showing that viewing a romantic partner had higher overall perceived support compared to a stranger before TBS administration ($P_{Bonf} = 0.001$). No other effect was observed ($P_s > 0.05$). Together, these results demonstrate an analgesic influence of social support in our protocol.

In the exploration of task difference in pain ratings following iTBS, the ANOVA revealed an interaction effect on pain ratings ($F_{1,19} = 9.24$, $P = 0.007$, $\eta_p^2 = 0.33$). Post-hoc test indicated that while pain was lower when viewing a romantic partner compared to a stranger before iTBS ($P_{Bonf} = 0.022$), the difference was significantly larger following iTBS ($P_{Bonf} = 0.001$). This result was driven by a significant increase in pain ($P_{Bonf} = 0.002$) in the stranger condition post-iTBS (Mean $_{\text{Pre-Partner}} = 30.18$; Mean $_{\text{Pre-Stranger}} = 34.60$; Mean $_{\text{Post-Partner}} = 29.43$; Mean $_{\text{Post-Stranger}} = 39.28$).

In the partner condition, the ANOVA revealed a main effect of time on overall perceived support ($F_{1,19} = 6.54$, $P = 0.019$, $\eta_p^2 = 0.26$), with post-hoc test showing that overall perceived support decreased from Pre-to Post-stimulation across TBS conditions ($P_{Bonf} = 0.019$) (*Supplementary Material S3*). No effect was observed in the stranger condition ($P_s > 0.05$).

4. Discussion

Previous studies have indicated that the mPFC plays a key role in mediating the analgesic effects of social support (Eisenberger et al., 2011; Younger et al., 2010). This study was designed to modulate dmPFC activity and related networks to investigate their role in mediating the

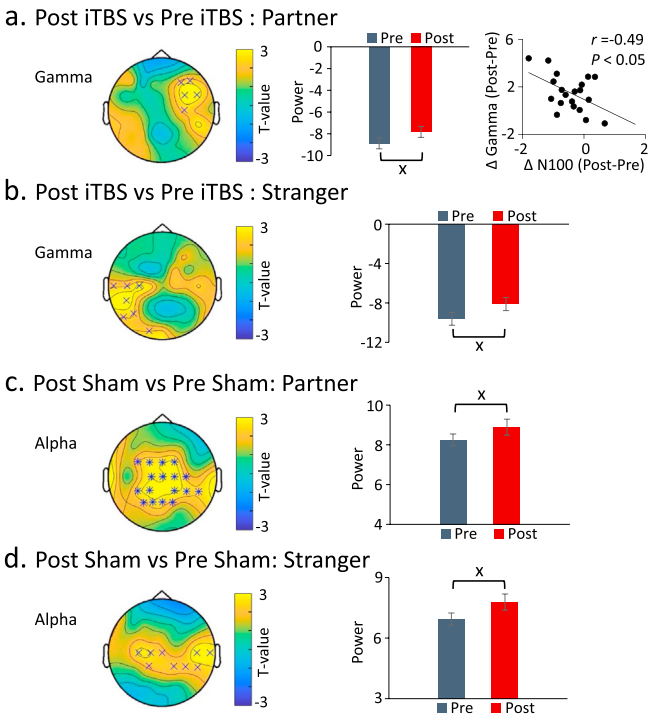

Fig. 5. Modulation of EEG oscillations by different TBS protocols. (a) iTBS increased fronto-central gamma power in the romantic partner condition (significant at F4, F6, FC4, FC6, and C4) (*left and middle panel*). Increased gamma activity was associated with larger N100 amplitude from Pre-to Post-iTBS (*right panel*). (b) iTBS increased central-parietal gamma power in the stranger condition (significant at T7, C5, C3, CP5, P7, P5 and O1). (c)–(d) show the increased central alpha power in the romantic partner and stranger condition respectively from Pre-to Post-Sham stimulation. Power is expressed as $10*\log_{10}$ (μV^2/Hz). X indicates $P < 0.05$, * indicates $P < 0.01$.

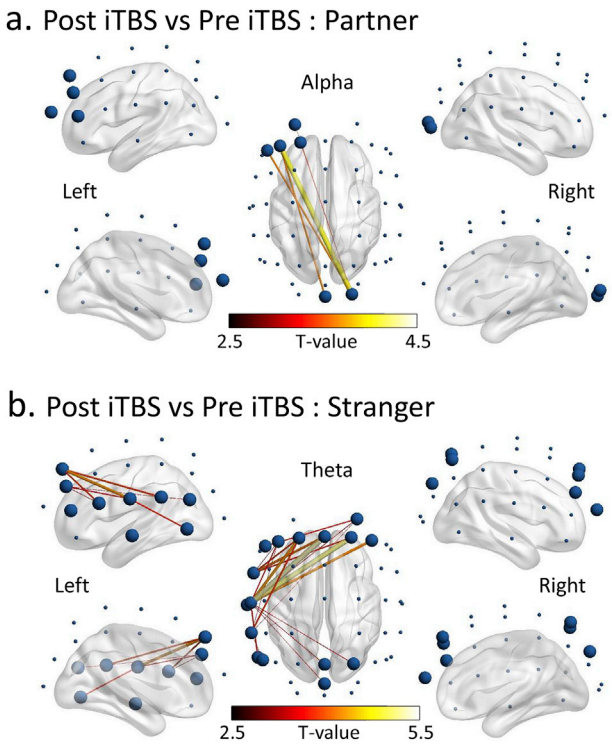

Fig. 6. EEG connectivity modulated by TBS protocols. (a) iTBS increased fronto-occipital alpha connectivity in the romantic partner condition. (b) In the stranger condition, iTBS increased central-frontal and central-parietal theta connectivity. Large dots highlight the significant electrodes, and the color and thickness of the lines indicate the T statistics.

influence of different social support contexts on pain experience. In line with previous observations, pain reduction was greater with social support from a romantic partner compared to stranger. Our data indicate that while iTBS elicited typical changes in TMS-EEG measures of neural activity at rest, it differentially influenced network connectivity and behavior across social support contexts. In line with other recent studies, cTBS and Sham stimulation did not elicit prominent changes. In sum, these findings provide novel evidence to support the role of dmPFC in the social modulation of pain.

Our baseline data indicate an analgesic influence of social support context which is consistent with previous studies (Che et al., 2017; Master et al., 2009; Younger et al., 2010). More specifically, pain was reduced when viewing a romantic partner compared to the stranger condition. This finding was consistently observed across three sessions. These findings add further evidence that visually presented social support can have an analgesic impact (Eisenberger et al., 2011; Younger et al., 2010).

With regard to the effects of TBS, it is important to firstly examine the efficacy of TBS conditions in modulating neural excitability, prior to considering behavioral and other effects. The neuroplastic effects of TBS delivered over non-motor regions such as the prefrontal cortex is most commonly quantified using TEPs. TEPs are suggested to reflect the shifts in the inhibition-excitation balance in cortical circuits following a single TMS pulse (Du et al., 2018; Rogasch and Fitzgerald, 2013). In this instance, we focused on N100 amplitude which is considered to be the most robust TEP component with the greatest signal-to-noise ratio (for discussion, see Cash et al., 2017; Noda et al., 2016). Furthermore, prior studies have identified N100 as being the component most reliably modulated by TBS (Chung et al., 2017, 2018b). While the auditory complex can overlap with N100 (Cash et al., 2017; Conde et al., 2019), there is no reason to expect that this would account for the differential modulation of N100 across TBS conditions. Furthermore, the intensity of single pulse TMS which elicits the N100 component was identical across conditions. While this is, to our knowledge, the first study to investigate the influence of TBS on dmPFC activity and connectivity using TMS-EEG, the increase in N100 amplitude by iTBS is consistent with the plastic changes observed when iTBS is delivered to other prefrontal regions (Fig. 4a) (Chung et al., 2017, 2018a), whereas there were no changes with cTBS or Sham stimulation (Fig. 4b–c). The absence of TEP changes with cTBS is in line with recent evidence which also observed more robust effects of iTBS compared to cTBS in modulating activity in prefrontal cortex (Chung et al., 2017, 2018b).

iTBS delivered to the dmPFC modulated the influence of social support on pain experience in a context-dependent fashion. The difference in baseline pain experience between romantic partner and stranger conditions was maintained and actually stronger following iTBS. ITBS therefore modified the interaction between social support context and pain experience. This selective and differential influence of dmPFC stimulation on pain experience according to social context was not evident in the Sham or cTBS conditions. Although we anticipated that stimulation of the dmPFC would modulate pain experience in the romantic partner condition, instead this condition appeared more robust to modulatory changes compared to the stranger condition. It is important to acknowledge that previous studies have indicated that both stranger and significant other conditions offer a degree of social support which typically reduces pain experience (Che et al., 2017; Roberts et al., 2015), including with visual representation of social support which was found to reduce affective experience of pain (Shaygan et al., 2017). Thus, while we had originally included the stranger condition as the control to the romantic other condition, it is possible that both conditions may provide a type of social support. The change in the stranger condition may either represent a reduction in pain alleviation by social support context or an increase in pain experience, while the romantic partner condition appeared more

resilient to perturbation. Future studies could further examine the effects of stimulation on the social modulation of pain, through comparison of additional control conditions including one without a social support context (see discussions in the limitation), and the inclusion of pain stimulus calibration. The causal modulation of the interaction between social support context and pain experience by dmPFC stimulation in the present study was accompanied by several clear changes in local and distributed network activity.

Pain and pain modulation are typically associated with distinct changes in neural activity, particularly in the gamma band (Peng et al., 2014). Our work extends these findings by demonstrating the modulation of pain related neural activity in the context of social support and the influence of dmPFC stimulation. Our data indicates that modulating dmPFC activity using iTBS increased fronto-central gamma activity in the romantic partner condition. These social context specific changes correlated with plastic changes in TEP amplitude following iTBS (Fig. 5a). In contrast, the stranger condition was associated with increased central-parietal gamma activity post iTBS (Fig. 5b). Gamma band activity is suggested to encode subjective pain experience (Nickel et al., 2017; Zhang et al., 2012). However, the increase in fronto-central gamma activity in the social support condition may otherwise reflect the role of gamma band activity in other higher-order cognitive processes, such as attention and the episodic memory retrieval (Canolty et al., 2006; Keizer et al., 2010; Marshall et al., 2015). One possibility is that the increase in fronto-central gamma activity following iTBS is related to attentional processing of visual social support and the retrieval of memory related to the romantic partner. The increase in gamma activity proximal to the stimulation site following excitatory stimulation at the prefrontal cortex is consistent with recent findings (Noda et al., 2017), however our data are the first to indicate a relationship between plastic changes in N100 amplitude and gamma activity linked to social support context.

In the stranger condition in which pain experience increased following iTBS, gamma activity was increased in central-parietal regions contralateral to the somatic site of pain delivery (Fig. 5b). This finding is consistent with previous studies which indicated gamma band activity in central-parietal cortical regions associated with somatosensory perception and pain integration (Hauck et al., 2015; Ploner et al., 2017; Zhang et al., 2012).

One of the most interesting aspects of our findings relates to the differential effects of dmPFC-TBS on network connectivity across different social support conditions. Connectivity across distributed neural regions typically manifests across lower frequencies, in particular the theta and alpha bands (Sauseng et al., 2010; Sauseng and Klimesch, 2008). In the romantic partner condition, but not the stranger condition, iTBS increased alpha band connectivity between frontal regions surrounding the stimulation site and occipital regions involved in visual processing (Fig. 6a). The romantic partner condition also appeared resilient to the increase in pain that was evident in the stranger condition following iTBS. This increase in alpha band connectivity appears consistent with previous evidence identifying a specific role of alpha band connectivity in mediating social support analgesia (Goldstein et al., 2018). Alpha band connectivity has also been implicated in other forms of social interaction (Dumas et al., 2010; Tognoli et al., 2007). Further evidence suggested that alpha coupling was positively associated with empathetic accuracy, the ability to understand others' feelings (Goldstein et al., 2018). Our finding extends the literature by indicating that alpha coupling between frontal and occipital regions may be involved in mediating the effects of visually presented social support information. The increased alpha coupling between frontal and occipital regions, apparently bypassing inclusion of intermediate sensory integration regions (in contrast to the stranger condition), could potentially represent the critical influence of visual input relating to social support from the romantic partner to frontal regions involved in social support (Eisenberger et al., 2011; Younger et al., 2010) and pain processing (Napadow et al., 2009), although this requires further investigation.

In contrast, iTBS over the dmPFC led to distributed changes in theta connectivity in the stranger condition. Specifically, connectivity was increased between left central regions associated with sensory processing of the pain stimulus, frontal regions near the TBS stimulation site and parietal regions likely involved in the integration of pain-related information (Fig. 6b). Previous evidence has identified a specific role of theta connectivity in relation to pain experience in which painful stimuli increased theta connectivity between central cortex and the parietal and frontal cortices in healthy individuals (Taesler and Rose, 2016). Moreover, we found increased coupling between temporal (as indicated by T7 electrode) and frontal regions, in which the temporal cortex plays a key role in understanding the intention of others (Allison et al., 2000; Pelphrey et al., 2004). In sum, it appears that stimulation of the dmPFC using iTBS is able to enhance the neural signatures associated with social support context and pain experience. It is worth emphasizing that these changes occurred in a single session, dmPFC-iTBS thus upregulated connectivity within specific networks in a context dependent fashion. These relationships could be causally investigated in future studies using transcranial alternating current stimulation which has the capacity to upregulate connectivity within specific frequency bands. Overall, these current findings provide evidence that the dmPFC has the capacity to orchestrate and modulate the effects associated with social support and pain across distributed brain regions.

In contrast to iTBS, cTBS did not demonstrate any changes in cortical plasticity (Fig. 4b), pain experience (Fig. 3b and f) or neural activity. This is consistent with the literature which suggests that cTBS is less effective in modulating brain activity compared to iTBS (Berlim et al., 2017; Chung et al., 2017). However, we did observe an increase in alpha power following Sham stimulation independent of the image type (Fig. 5c and d). Pain has been shown to suppress alpha activity which is related to nociceptive attention (Nickel et al., 2017; Peng et al., 2014). Conversely, increased alpha activity is associated with cortical "deactivation" and is sometimes referred to as an 'idling' state (Cash et al., 2017; Jensen and Mazaheri, 2010). Increased alpha activity post Sham stimulation therefore may suggest less attention driven by the painful stimuli or the social support information as the participants knew what to expect from Pre-to Post-stimulation.

Findings of the current study improves our understanding of the mechanisms that may mediate the influence of social support context on pain. Using TBS, activity of the dmPFC was temporarily modulated which allowed the investigatation of its causal role in the processing of social support as well as the influence on pain experience. Moreover, TMS-EEG has the capacity to assess neural plasticity changes caused by TBS. Combination of these techniques would supplement in generating stronger conclusions surrounding social support and pain. Furthermore, the current study provides evidence beyond local brain activation, which extends the literature to understand the neural networks and dynamics surrounding the impact of social support context on pain. Overall, our findings may help to understand the potential therapeutic influence of social support in the management of pain whereby empirical evidence is limited surrounding the social contexts and mechanisms of the pain-relieving effect of social support (Keefe et al., 1996, 1999).

We acknowledge some limitations with the current study. We only used one image of the romantic partner whereby a consistent reduction in perceived social support across sessions was evident, independent of TBS condition (*Supplementary Material S3*). Habituation to the image may have influenced the capacity to elicit reductions in pain experience in the romantic partner condition following iTBS. Future studies would benefit from using multiple images that have the same valence to the support recipient. Secondly, we did not include an inanimate object control condition in the pain task. This could have provided a more neutral condition, compared to the stranger, as has been used in other comparative investigations (e.g. Eisenberger et al., 2011). Future studies may wish to incorporate an additional condition where no other person is present to further interrogate the effects of social support, including our finding of increased pain in the stranger condition following iTBS. The TMS coil was positioned based on F1 electrode location. Electrode-based

positioning is commonly employed in TMS-EEG research (Cash et al., 2017; Chung et al., 2018c) and similar to the F3 approach used in the treatment of clinical disorders (Beam et al., 2009). However, it is not as accurate as MRI-guided neuronavigation which was not feasible in the present study. Moreover, we only targeted the left dmPFC based on fMRI evidence identifying the left mPFC activation in social support analgesia (Eisenberger et al., 2011; Younger et al., 2010). These findings could be complemented in future studies by different sessions targeting and examining left and right dmPFC. Given the rapid decay of magnetic fields with distance from the source, it would also be difficult to preferentially target deeper regions using standard TMS (Deng et al., 2013). Neural and behavioral modulation might also be enhanced in future studies using other recently developed individualized TMS protocols (Cash et al., 2014; Chung et al., 2018c).

In conclusion, this study used TBS together with EEG and TMS-EEG to investigate the role of dmPFC and associated networks in mediating the influence of social support context on pain. Our data demonstrated neural plasticity changes in the prefrontal cortex, which was associated with increased pain experience at the subjective and neural level in the context of viewing a stranger. In contrast, social support context was associated with distinct neural activity and connectivity that could be modulated by plasticity changes in the prefrontal cortex. As such, it seems that stimulation of the dmPFC can flexibly elicit context-dependent behavioral and brain connectivity changes surrounding social support and pain. Overall, our findings appear to support a key role of the dmPFC in regulating local and distributed brain activities to the social modulation of pain.

Author contributions

XC, RC, and BF contributed to the experimental design, data collection and analysis, and manuscript preparation. PF contributed to the experimental design and manuscript preparation. SC and NB contributed to the data analysis and manuscript preparation.

Disclosures

This work was supported by the China Scholarship Council; the NHMRC Practitioner.

Fellowship (606907), and the NHMRC Early Career Fellowship. The authors declare no competing financial interests.

Appendix A. Supplementary data

Supplementary data to this article can be found online at https://doi.org/10.1016/j.neuroimage.2019.116053.

References

Allison, T., Puce, A., McCarthy, G., 2000. Social perception from visual cues: role of the STS region. Trends Cogn. Sci. 4, 267–278.

Apkarian, A.V., Bushnell, M.C., Treede, R.-D., Zubieta, J.-K., 2005. Human brain mechanisms of pain perception and regulation in health and disease. Eur. J. Pain 9, 463–484.

Bailey, N., Hoy, K., Rogasch, N., Thomson, R., McQueen, S., Elliot, D., Sullivan, C., Fulcher, B., Daskalakis, Z., Fitzgerald, P., 2018. Responders to rTMS for depression show increased fronto-midline theta and theta connectivity compared to non-responders. Brain Stimul. 11, 190–203.

Beam, W., Borckardt, J.J., Reeves, S.T., George, M.S., 2009. An efficient and accurate new method for locating the F3 position for prefrontal TMS applications. Brain Stimul. 2, 50–54.

Berlim, M.T., McGirr, A., dos Santos, N.R., Tremblay, S., Martins, R., 2017. Efficacy of theta burst stimulation (TBS) for major depression: an exploratory meta-analysis of randomized and sham-controlled trials. J. Psychiatr. Res. 90, 102–109.

Bzdok, D., Schilbach, L., Vogeley, K., Schneider, K., Laird, A.R., Langner, R., Eickhoff, S.B., 2012. Parsing the neural correlates of moral cognition: ALE meta-analysis on morality, theory of mind, and empathy. Brain Struct. Funct. 217, 783–796.

Canolty, R.T., Edwards, E., Dalal, S.S., Soltani, M., Nagarajan, S.S., Kirsch, H.E., Berger, M.S., Barbaro, N.M., Knight, R.T., 2006. High gamma power is phase-locked to theta oscillations in human neocortex. Science 313, 1626–1628.

Cash, R.F., Murakami, T., Chen, R., Thickbroom, G.W., Ziemann, U., 2014. Augmenting plasticity induction in human motor cortex by disinhibition stimulation. Cerebr. Cortex 26, 58–69.

Cash, R.F., Noda, Y., Zomorrodi, R., Radhu, N., Farzan, F., Rajji, T.K., Fitzgerald, P.B., Chen, R., Daskalakis, Z.J., Blumberger, D.M., 2017. Characterization of glutamatergic and GABA A-mediated neurotransmission in motor and dorsolateral prefrontal cortex using paired-pulse TMS–EEG. Neuropsychopharmacology 42, 502–511.

Che, X., Cash, R., Chung, S.W., Fitzgerald, P., Fitzgibbon, B.M., 2018a. Investigating the influence of social support on experimental pain and related physiological arousal: a systematic review and meta-analysis. Neurosci. Biobehav. Rev. 92, 437–452.

Che, X., Cash, R., Fitzgerald, P., Fitzgibbon, B.M., 2017. The social regulation of pain: autonomic and neurophysiological changes associated with perceived threat. J. Pain 19, 496–505.

Che, X., Cash, R., Ng, S.K., Fitzgerald, P., Fitzgibbon, B.M., 2018b. A systematic review of the processes underlying the main and the buffering effect of social support on the experience of pain. Clin. J. Pain 34, 1061–1076.

Che, X., Zhang, Q., Zhao, J., Wei, D., Li, B., Guo, Y., Qiu, J., Liu, Y., 2014. Synchronous activation within the default mode network correlates with perceived social support. Neuropsychologia 63, 26–33.

Chung, S.W., Lewis, B.P., Rogasch, N.C., Saeki, T., Thomson, R.H., Hoy, K.E., Bailey, N.W., Fitzgerald, P.B., 2017. Demonstration of short-term plasticity in the dorsolateral prefrontal cortex with theta burst stimulation: a TMS-EEG study. Clin. Neurophysiol. 128, 1117–1126.

Chung, S.W., Rogasch, N.C., Hoy, K.E., Fitzgerald, P.B., 2015. Measuring brain stimulation induced changes in cortical properties using TMS-EEG. Brain Stimul. 8, 1010–1020.

Chung, S.W., Rogasch, N.C., Hoy, K.E., Fitzgerald, P.B., 2018a. The effect of single and repeated prefrontal intermittent theta burst stimulation on cortical reactivity and working memory. Brain Stimul. 11, 566–574.

Chung, S.W., Rogasch, N.C., Hoy, K.E., Sullivan, C.M., Cash, R.F., Fitzgerald, P.B., 2018b. Impact of different intensities of intermittent theta burst stimulation on the cortical properties during TMS-EEG and working memory performance. Hum. Brain Mapp. 39, 783–802.

Chung, S.W., Sullivan, C.M., Rogasch, N.C., Hoy, K.E., Bailey, N.W., Cash, R.F., Fitzgerald, P.B., 2018c. The effects of individualised intermittent theta burst stimulation in the prefrontal cortex: a TMS-EEG study. Hum. Brain Mapp. 40, 608–627.

Conde, V., Tomasevic, L., Akopian, I., Stanek, K., Saturnino, G.B., Thielscher, A., Bergmann, T.O., Siebner, H.R., 2019. The non-transcranial TMS-evoked potential is an inherent source of ambiguity in TMS-EEG studies. Neuroimage 185, 300–312.

Conforto, A.B., Z'Graggen, W.J., Kohl, A.S., Rösler, K.M., Kaelin-Lang, A., 2004. Impact of coil position and electrophysiological monitoring on determination of motor thresholds to transcranial magnetic stimulation. Clin. Neurophysiol. 115, 812–819.

Delorme, A., Makeig, S., 2004. EEGLAB: an open source toolbox for analysis of single-trial EEG dynamics including independent component analysis. J. Neurosci. Methods 134, 9–21.

Deng, Z.-D., Lisanby, S.H., Peterchev, A.V., 2013. Electric field depth–focality tradeoff in transcranial magnetic stimulation: simulation comparison of 50 coil designs. Brain Stimul. 6, 1–13.

Downar, J., Sankar, A., Giacobbe, P., Woodside, B., Colton, P., 2012. Unanticipated rapid remission of refractory bulimia nervosa, during high-dose repetitive transcranial magnetic stimulation of the dorsomedial prefrontal cortex: a case report. Front. Psychiatry 3, e30.

Du, X., Rowland, L.M., Summerfelt, A., Wijtenburg, S.A., Chiappelli, J., Wisner, K., Kochunov, P., Choa, F.-S., Hong, L.E., 2018. TMS evoked N100 reflects local GABA and glutamate balance. Brain Stimul. 11, 1071–1079.

Dumas, G., Nadel, J., Soussignan, R., Martinerie, J., Garnero, L., 2010. Inter-brain synchronization during social interaction. PLoS One 5, e12166.

Dunkel-Schetter, C., Bennett, T.L., 1990. Differentiating the cognitive and behavioral aspects of social support. In: Sarason, B.R., Sarason, I.G., Pierce, G.R. (Eds.), Wiley Series on Personality Processes. Social Support: an Interactional View. John Wiley, Oxford, pp. 267–296.

Eisenberger, N.I., Master, S.L., Inagaki, T.K., Taylor, S.E., Shirinyan, D., Lieberman, M.D., Naliboff, B.D., 2011. Attachment figures activate a safety signal-related neural region and reduce pain experience. Proc. Natl. Acad. Sci. 108, 11721–11726.

Fox, M.D., Snyder, A.Z., Vincent, J.L., Corbetta, M., Van Essen, D.C., Raichle, M.E., 2005. The human brain is intrinsically organized into dynamic, anticorrelated functional networks. Proc. Natl. Acad. Sci. 102, 9673–9678.

Fuggetta, G., Fiaschi, A., Manganotti, P., 2005. Modulation of cortical oscillatory activities induced by varying single-pulse transcranial magnetic stimulation intensity over the left primary motor area: a combined EEG and TMS study. Neuroimage 27, 896–908.

Furman, A.J., Meeker, T.J., Rietschel, J.C., Yoo, S., Muthulingam, J., Prokhorenko, M., Keaser, M.L., Goodman, R.N., Mazaheri, A., Seminowicz, D.A., 2018. Cerebral peak alpha frequency predicts individual differences in pain sensitivity. Neuroimage 167, 203–210.

Gamond, L., Cattaneo, Z., 2016. The dorsomedial prefrontal cortex plays a causal role in mediating in-group advantage in emotion recognition: a TMS study. Neuropsychologia 93, 312–317.

Gamond, L., Ferrari, C., La Rocca, S., Cattaneo, Z., 2017. Dorsomedial prefrontal cortex and cerebellar contribution to in-group attitudes: a transcranial magnetic stimulation study. Eur. J. Neurosci. 45, 932–939.

Geuzaine, C., Remacle, J.F., 2009. Gmsh: a 3-D finite element mesh generator with built-in pre-and post-processing facilities. Int. J. Numer. Methods Eng. 79, 1309–1331.

Goldstein, P., Shamay-Tsoory, S.G., Yellinek, S., Weissman-Fogel, I., 2016. Empathy predicts an experimental pain reduction during touch. J. Pain 17, 1049–1057.

Goldstein, P., Weissman-Fogel, I., Dumas, G., Shamay-Tsoory, S.G., 2018. Brain-to-brain coupling during handholding is associated with pain reduction. Proc. Natl. Acad. Sci. 115, E2528–E2537.
Goldsworthy, M.R., Pitcher, J.B., Ridding, M.C., 2012. The application of spaced theta burst protocols induces long-lasting neuroplastic changes in the human motor cortex. Eur. J. Neurosci. 35, 125–134.
Gramfort, A., Papadopoulo, T., Olivi, E., Clerc, M., 2010. OpenMEEG: opensource software for quasistatic bioelectromagnetics. Biomed. Eng. Online 9, e45.
Hadjileontiadis, L.J., 2015. EEG-based tonic cold pain characterization using wavelet higher order spectral features. IEEE (Inst. Electr. Electron. Eng.) Trans. Biomed. Eng. 62, 1981–1991.
Hardmeier, M., Hatz, F., Bousleiman, H., Schindler, C., Stam, C.J., Fuhr, P., 2014. Reproducibility of functional connectivity and graph measures based on the phase lag index (PLI) and weighted phase lag index (wPLI) derived from high resolution EEG. PLoS One 9, e108648.
Hauck, M., Lorenz, J., Domnick, C., Gerloff, C., Engel, A.K., 2015. Top-down and bottom-up modulation of pain-induced oscillations. Front. Hum. Neurosci. 9, e375.
Hill, A.T., Rogasch, N.C., Fitzgerald, P.B., Hoy, K.E., 2017. Effects of prefrontal bipolar and high-definition transcranial direct current stimulation on cortical reactivity and working memory in healthy adults. Neuroimage 152, 142–157.
Huang, Y.-Z., Edwards, M.J., Rounis, E., Bhatia, K.P., Rothwell, J.C., 2005. Theta burst stimulation of the human motor cortex. Neuron 45, 201–206.
Iwabuchi, S.J., Raschke, F., Auer, D.P., Liddle, P.F., Lankappa, S.T., Palaniyappan, L., 2017. Targeted transcranial theta-burst stimulation alters fronto-insular network and prefrontal GABA. Neuroimage 146, 395–403.
Jensen, O., Mazaheri, A., 2010. Shaping functional architecture by oscillatory alpha activity: gating by inhibition. Front. Hum. Neurosci. 4, e186.
Keefe, F.J., Caldwell, D.S., Baucom, D., Salley, A., Robinson, E., Timmons, K., Beaupre, P., Weisberg, J., Helms, M., 1996. Spouse-assisted coping skills training in the management of osteoarthritic knee pain. Arthritis Rheumatol. 9, 279–291.
Keefe, F.J., Caldwell, D.S., Baucom, D., Salley, A., Robinson, E., Timmons, K., Beaupre, P., Weisberg, J., Helms, M., 1999. Spouse-assisted coping skills training in the management of knee pain in osteoarthritis: long-term followup results. Arthritis Rheum. 12, 101–111.
Keizer, A.W., Verment, R.S., Hommel, B., 2010. Enhancing cognitive control through neurofeedback: a role of gamma-band activity in managing episodic retrieval. Neuroimage 49, 3404–3413.
Koessler, L., Maillard, L., Benhadid, A., Vignal, J.P., Felblinger, J., Vespignani, H., Braun, M., 2009. Automated cortical projection of EEG sensors: anatomical correlation via the international 10–10 system. Neuroimage 46, 64–72.
Korhonen, R.J., Hernandez-Pavon, J.C., Metsomaa, J., Mäki, H., Ilmoniemi, R.J., Sarvas, J., 2011. Removal of large muscle artifacts from transcranial magnetic stimulation-evoked EEG by independent component analysis. Med. Biol. Eng. Comput. 49, 397–407.
Krahé, C., Springer, A., Weinman, J.A., Fotopoulou, A., 2013. The social modulation of pain: others as predictive signals of salience–a systematic review. Front. Hum. Neurosci. 7, e386.
Kucyi, A., Salomons, T.V., Davis, K.D., 2013. Mind wandering away from pain dynamically engages antinociceptive and default mode brain networks. Proc. Natl. Acad. Sci. 110, 18692–18697.
Lin, F.H., Belliveau, J.W., Dale, A.M., Hämäläinen, M.S., 2006. Distributed current estimates using cortical orientation constraints. Hum. Brain Mapp. 27, 1–13.
Maris, E., Oostenveld, R., 2007. Nonparametric statistical testing of EEG-and MEG-data. J. Neurosci. Methods 164, 177–190.
Marshall, T.R., O'Shea, J., Jensen, O., Bergmann, T.O., 2015. Frontal eye fields control attentional modulation of alpha and gamma oscillations in contralateral occipitoparietal cortex. J. Neurosci. 35, 1638–1647.
Master, S.L., Eisenberger, N.I., Taylor, S.E., Naliboff, B.D., Shirinyan, D., Lieberman, M.D., 2009. A picture's worth: partner photographs reduce experimentally induced pain. Psychol. Sci. 20, 1316–1318.
Napadow, V., Dhond, R.P., Kim, J., LaCount, L., Vangel, M., Harris, R.E., Kettner, N., Park, K., 2009. Brain encoding of acupuncture sensation—coupling on-line rating with fMRI. Neuroimage 47, 1055–1065.
Ni, Z., Gunraj, C., Kailey, P., Cash, R.F., Chen, R., 2014. Heterosynaptic modulation of motor cortical plasticity in human. J. Neurosci. 34, 7314–7321.
Nickel, M.M., May, E.S., Tiemann, L., Schmidt, P., Postorino, M., Dinh, S.T., Gross, J., Ploner, M., 2017. Brain oscillations differentially encode noxious stimulus intensity and pain intensity. Neuroimage 148, 141–147.
Nikouline, V., Ruohonen, J., Ilmoniemi, R.J., 1999. The role of the coil click in TMS assessed with simultaneous EEG. Clin. Neurophysiol. 110, 1325–1328.
Nikulin, V.V., Kičić, D., Kähkönen, S., Ilmoniemi, R.J., 2003. Modulation of electroencephalographic responses to transcranial magnetic stimulation: evidence for changes in cortical excitability related to movement. Eur. J. Neurosci. 18, 1206–1212.
Noda, Y., Cash, R.F., Zomorrodi, R., Dominguez, L.G., Farzan, F., Rajji, T.K., Barr, M.S., Chen, R., Daskalakis, Z.J., Blumberger, D.M., 2016. A combined TMS-EEG study of short-latency afferent inhibition in the motor and dorsolateral prefrontal cortex. J. Neurophysiol. 116, 938–948.
Noda, Y., Zomorrodi, R., Saeki, T., Rajji, T.K., Blumberger, D.M., Daskalakis, Z.J., Nakamura, M., 2017. Resting-state EEG gamma power and theta–gamma coupling enhancement following high-frequency left dorsolateral prefrontal rTMS in patients with depression. Clin. Neurophysiol. 128, 424–432.
Oostenveld, R., Fries, P., Maris, E., Schoffelen, J.-M., 2011. FieldTrip: open source software for advanced analysis of MEG, EEG, and invasive electrophysiological data. Comput. Intell. Neurosci. 2011, e1.
Parsons, C.E., Young, K.S., Mohseni, H., Woolrich, M.W., Thomsen, K.R., Joensson, M., Murray, L., Goodacre, T., Stein, A., Kringelbach, M.L., 2013. Minor structural abnormalities in the infant face disrupt neural processing: a unique window into early caregiving responses. Soc. Neurosci. 8, 268–274.
Pelphrey, K.A., Morris, J.P., Mccarthy, G., 2004. Grasping the intentions of others: the perceived intentionality of an action influences activity in the superior temporal sulcus during social perception. J. Cogn. Neurosci. 16, 1706–1716.
Peng, W., Hu, L., Zhang, Z., Hu, Y., 2014. Changes of spontaneous oscillatory activity to tonic heat pain. PLoS One 9, e91052.
Peyron, R., García-Larrea, L., Grégoire, M.-C., Costes, N., Convers, P., Lavenne, F., Mauguière, F., Michel, D., Laurent, B., 1999. Haemodynamic brain responses to acute pain in humans: sensory and attentional networks. Brain 122, 1765–1780.
Ploner, M., Sorg, C., Gross, J., 2017. Brain rhythms of pain. Trends Cogn. Sci. 21, 100–110.
Rastogi, A., Cash, R., Dunlop, K., Vesia, M., Kucyi, A., Ghahremani, A., Downar, J., Chen, J., Chen, R., 2017. Modulation of cognitive cerebello-cerebral functional connectivity by lateral cerebellar continuous theta burst stimulation. Neuroimage 158, 48–57.
Roberts, M.H., Klatzkin, R.R., Mechlin, B., 2015. Social support attenuates physiological stress responses and experimental pain sensitivity to cold pressor pain. Ann. Behav. Med. 49, 557–569.
Rogasch, N.C., Fitzgerald, P.B., 2013. Assessing cortical network properties using TMS–EEG. Hum. Brain Mapp. 34, 1652–1669.
Rogasch, N.C., Sullivan, C., Thomson, R.H., Rose, N.S., Bailey, N.W., Fitzgerald, P.B., Farzan, F., Hernandez-Pavon, J.C., 2017. Analysing concurrent transcranial magnetic stimulation and electroencephalographic data: a review and introduction to the open-source TESA software. Neuroimage 147, 934–951.
Rogasch, N.C., Thomson, R.H., Daskalakis, Z.J., Fitzgerald, P.B., 2013. Short-latency artifacts associated with concurrent TMS–EEG. Brain Stimul. 6, 868–876.
Rogasch, N.C., Thomson, R.H., Farzan, F., Fitzgibbon, B.M., Bailey, N.W., Hernandez-Pavon, J.C., Daskalakis, Z.J., Fitzgerald, P.B., 2014. Removing artefacts from TMS-EEG recordings using independent component analysis: importance for assessing prefrontal and motor cortex network properties. Neuroimage 101, 425–439.
Salomons, T.V., Dunlop, K., Kennedy, S.H., Flint, A., Geraci, J., Giacobbe, P., Downar, J., 2014. Resting-state cortico-thalamic-striatal connectivity predicts response to dorsomedial prefrontal rTMS in major depressive disorder. Neuropsychopharmacology 39, 488–498.
Sauseng, P., Griesmayr, B., Freunberger, R., Klimesch, W., 2010. Control mechanisms in working memory: a possible function of EEG theta oscillations. Neurosci. Biobehav. Rev. 34, 1015–1022.
Sauseng, P., Klimesch, W., 2008. What does phase information of oscillatory brain activity tell us about cognitive processes? Neurosci. Biobehav. Rev. 32, 1001–1013.
Schulz, E., May, E.S., Postorino, M., Tiemann, L., Nickel, M.M., Witkovsky, V., Schmidt, P., Gross, J., Ploner, M., 2015. Prefrontal gamma oscillations encode tonic pain in humans. Cerebr. Cortex 25, 4407–4414.
Schuwerk, T., Schecklmann, M., Langguth, B., Döhnel, K., Sodian, B., Sommer, M., 2014. Inhibiting the posterior medial prefrontal cortex by rTMS decreases the discrepancy between self and other in theory of mind reasoning. Behav. Brain Res. 274, 312–318.
Selesnick, I.W., Burrus, C.S., 1998. Generalized digital Butterworth filter design. IEEE Trans. Signal Process. 46, 1688–1694.
Shaygan, M., Böger, A., Kröner-Herwig, B., 2017. Valence and arousal value of visual stimuli and their role in the mitigation of chronic pain: what is the power of pictures? J. Pain 18, 124–131.
Sheehan, D., Lecrubier, Y., 2001. MINI SCREEN 5.0. 0/English Version/DSM-IV July/1/06. University of South Florida-TAMPA, Florida.
Tadel, F., Baillet, S., Mosher, J.C., Pantazis, D., Leahy, R.M., 2011. Brainstorm: a user-friendly application for MEG/EEG analysis. Comput. Intell. Neurosci. 2011, e8.
Taesler, P., Rose, M., 2016. Prestimulus theta oscillations and connectivity modulate pain perception. J. Neurosci. 36, 5026–5033.
Tognoli, E., Lagarde, J., DeGuzman, G.C., Kelso, J.S., 2007. The phi complex as a neuromarker of human social coordination. Proc. Natl. Acad. Sci. 104, 8190–8195.
Vinck, M., Oostenveld, R., Van Wingerden, M., Battaglia, F., Pennartz, C.M., 2011. An improved index of phase-synchronization for electrophysiological data in the presence of volume-conduction, noise and sample-size bias. Neuroimage 55, 1548–1565.
Windhoff, M., Opitz, A., Thielscher, A., 2013. Electric field calculations in brain stimulation based on finite elements: an optimized processing pipeline for the generation and usage of accurate individual head models. Hum. Brain Mapp. 34, 923–935.
Younger, J., Aron, A., Parke, S., Chatterjee, N., Mackey, S., 2010. Viewing pictures of a romantic partner reduces experimental pain: involvement of neural reward systems. PLoS One 5, e13309.
Zalesky, A., Fornito, A., Bullmore, E.T., 2010. Network-based statistic: identifying differences in brain networks. Neuroimage 53, 1197–1207.
Zhang, Z., Hu, L., Hung, Y.S., Mouraux, A., Iannetti, G., 2012. Gamma-band oscillations in the primary somatosensory cortex—a direct and obligatory correlate of subjective pain intensity. J. Neurosci. 32, 7429–7438.